

## Precise measurements of ionic masses for QED tests

T. Fritioff<sup>a</sup>, I. Bergström<sup>b</sup>, Sz. Nagy<sup>a</sup>, A. Solders<sup>a</sup>, M. Suhonen<sup>a</sup>, R. Schuch<sup>a,\*</sup>

<sup>a</sup> Atomic Physics, AlbaNova, Stockholm University, S-106 91 Stockholm, Sweden

<sup>b</sup> Manne Siegbahn Laboratory (MSL), Frescativägen 24, S-104 05 Stockholm, Sweden

Received 17 December 2005; received in revised form 31 January 2006; accepted 6 February 2006

### Abstract

The Penning trap mass spectrometer SMILETRAP is designed for precision mass measurements using the merits of highly charged ions. In this paper we describe the feature of SMILETRAP and give examples of mass measurements involving  $^{24}\text{Mg}^{11+}$ ,  $^{26}\text{Mg}^{11+}$ ,  $^{40}\text{Ca}^{17+}$  and  $^{40}\text{Ca}^{19+}$  ions. These emphasize the importance of accurate masses of hydrogen-like and lithium-like ions that are required in the evaluation of  $g$ -factor measurements of electrons bound to even–even nuclei and test of QED effects. Highly precise mass measurements can also be used for testing atomic structure calculations and determining atomic binding energies. Relevance of such measurements throughout the periodic system is discussed. © 2006 Elsevier B.V. All rights reserved.

**Keywords:**  $g$ -Factor; Penning trap; Lamor precision frequency; Isotopes; QED

### 1. Introduction

The mass is a fundamental property of an atom. High-precision mass values have a wide range of applications in modern physics, including the determination of fundamental constants, verification of nuclear models, benchmark values in atomic mass tables, test of the standard model, test of QED, metrology, and other fields of fundamental physics [1].

The principle of mass measurements with Penning traps is the determination of the cyclotron frequency  $\nu_c = qeB/2\pi m$  of the ion, with charge  $q$ , trapped in the magnetic field  $B$ . Due to the long observation time and the well understood dynamics of the ion motion in a trap, Penning trap mass spectrometers are the leading devices in the field of high-accuracy mass spectrometry today. It is evident that the precision in the mass  $m$  increases linearly with  $q$ , since  $m/\Delta m = \nu/\Delta\nu$  increases linearly with  $\nu$  for a resonance width  $\Delta\nu$  given by a fixed observation time  $\Delta t$  (as  $\Delta\nu \sim 1/\Delta t$ ). SMILETRAP is the first Penning trap mass spectrometer that is designed for exploiting the mass precision increase by using highly charged ions.

SMILETRAP (Stockholm–Mainz Ion LEvitation TRAP) was set up in collaboration with the Physics Department of the Johannes Gutenberg University in Mainz, Germany. It is to a

great extent a copy of ISOLTRAP, another Penning trap mass spectrometer designed for mass measurements of radioactive atoms [2]. Into SMILETRAP, we inject highly charged ions for precision mass measurements. These come from an electron beam ion source, CRYISIS, which can deliver isotopically separated highly charged ion beams. The trap device consists of a cylindrical Penning trap, pre-trap, for retardation and preparation of the ions and a hyperbolic Penning trap, precision trap, for the cyclotron frequency measurement using the time-of-flight (TOF) technique [3]. This technique of injecting externally produced ions into the trap and extracting them for the resonance detection is used at ISOLTRAP and SMILETRAP. Also used in other experiments is the technique to measure the motional frequencies of internally produced trapped ions by detecting the image currents induced in the trap electrodes. This approach has the advantage of cooling the ion resistively by coupling its motion to the detection system. We apply a different method to get a rather cold ion into SMILETRAP. First we select the coldest ions on the beam transport. Then, we evaporate the hottest ions by boil-off, first in the pre-trap and then in the precision trap. The advantage of our technique is that it allows for a rapid change between the ion of interest and a reference ion. It also makes it possible to vary the ion charge state  $q$  in one set of measurements, allowing for systematic error check, and, as we will discuss later, for atomic binding energy determinations by measuring different charge states of the same atom.

\* Corresponding author.

E-mail address: [schuch@physto.se](mailto:schuch@physto.se) (Schuch).

So far, mass measurements involving ions of about 30 isotopes in the mass range 1–200 u and charges from 1+ to 52+ have been performed at SMILETRAP [4]. Among the highlights are the determination of the  $^{76}\text{Ge}$  double  $\beta$ -decay  $Q$ -value [5] and the mass measurement of  $^{133}\text{Cs}$  related to the determination of a new value for the fine structure constant  $\alpha$  [6]. The mass of the  $^{28}\text{Si}$  was measured which is related to a possible atomic definition of the kg-standard [7]. By measuring the mass of the  $^{198}\text{Hg}$  and  $^{204}\text{Hg}$ , a problem in the atomic mass table has been solved [8]. Very recently, by adding a new mass measurement involving  $^3\text{He}^{1+}$  ions we improved our previous  $Q$ -value for the tritium  $\beta$ -decay by a factor of 2, resulting in an uncertainty of 1.2 eV, thus being presently the most accurate  $Q$ -value, and more importantly, it is based on correct atomic masses [9]. A new mass value for  $^7\text{Li}$  has been measured, to be used as mass calibration at ISOLTRAP when measuring the masses of halo nuclei of He and Li [10].

In the following we show examples of accurate ionic mass measurements of highly charged ions for determining the  $g$ -factor of the bound electron. We shall also discuss the possibility of using these measurements for testing QED effects of strongly bound electrons and how precise ionic mass measurements can be used to determine electron binding energies and weigh QED effects directly.

## 2. Experimental procedure of mass measurements with SMILETRAP

The SMILETRAP facility has been described in detail in Ref. [4], thus only a brief description will be given here.

In order to have access to a wide variety of highly charged ions an electron beam ion source (CRYSIS), in combination with an external ion injector is used [11]. In order to produce an isotopically clean beam of highly charged ions, singly charged ions are created in the external ion source from gas, by evaporation from an oven or by sputtering. The extracted singly charged ions are mass separated and injected into CRYSIS for charge breeding. The low abundances of certain elements can be compensated for by producing intense beams of 1+ ions and by increasing the injection time. The confinement time, i.e., the time the ions are exposed to the electron impact ionization inside the source, and the electron beam energy can be varied to optimize the desired charge state. The extracted ion pulse is transported to the double Penning trap system by use of conventional electrostatic ion beam optics. Before entering the cylindrical retardation trap (pre-trap) the ions are charge state selected in a  $90^\circ$  double-focusing magnet. The pre-trap is used to retard the ions from the transportation energy of typically  $3.4q$  keV to ground potential within 30 ms. The ions are accelerated again by  $-1$  kV and are transported to the hyperboloidal precision Penning trap where they are finally retarded to ground potential and captured. An aperture with 1 mm diameter prevents ions with too large radii to enter the precision trap. The trapped ions are subject to an evaporation process by lowering the trap voltage from 5 to 0.1 V leaving only the coldest ions in the trap. In average not more than 1–2 ions are left in the precision trap after this procedure.

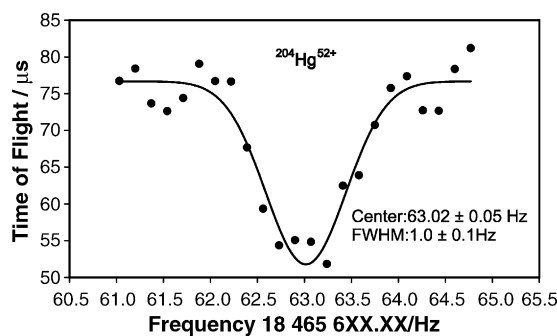


Fig. 1. A typical cyclotron frequency resonance in the time-of-flight of  $\text{Hg}^{52+}$  ions measured with SMILETRAP.

The precision Penning trap is located in the homogeneous magnetic field of a superconducting solenoid ( $B = 4.7$  T). It consists of a ring electrode and two end-cap electrodes all with hyperboloidal geometry which create an electrostatic quadrupole field. In this combined magnetic and electric field the ion motion can be described by three well defined eigenmotions [12]; an axial motion with frequency  $\nu_z$ , the so-called magnetron motion with frequency  $\nu_-$  and the reduced cyclotron motion with frequency  $\nu_+$ . The two radial frequencies obey the relation  $\nu_c = \nu_- + \nu_+$ .

The mass measurement is carried out via the determination of the cyclotron frequency  $\nu_c = qB/2\pi m$  of the ion stored in the Penning trap. The cyclotron frequency is probed by exciting the ion motion by a quadrupolar radio frequency signal (rf) and a subsequent measurement of the time-of-flight to the micro-channel-plate detector placed on top of the magnet [13,4]. Repeating this procedure for different rf frequencies around the true cyclotron frequency  $\nu_c$  and measuring the time-of-flight as a function of the rf frequency, yields a characteristic time-of-flight cyclotron frequency resonance curve [13]. In order to obtain the ionic mass from the measured frequency, the magnetic field has to be calibrated. This is done by the measurement of the cyclotron frequency  $\nu_c^{\text{ref}}$  of a reference ion with well-known mass. The two measurements are performed almost simultaneously in order to minimize effects from  $B$ -field variations.

The mass of the reference ion  $m(\text{H}_2^+) = 2.01510149703$  (27) u has a relative uncertainty of 0.14 ppb [4]. It is produced in the preparation trap by bombarding the rest gas with 3.4 keV electrons. The measurements are performed by using a continuous excitation time  $T_{\text{rf}}$  of 1 s. A time-of-flight cyclotron frequency resonance measured with  $\text{Hg}^{52+}$  ions is shown in Fig. 1, showing that the time-of-flight method works well for highly charged ions.

The expected sidebands of the resonance [13] are indicated in the measured distribution. They are not included in the fit because they are often suppressed. This is mainly due to an initial spread of magnetron/cyclotron radii, an incomplete conversion of magnetron into reduced cyclotron motion during excitation and a fast oscillation of the magnetic field due to our field stabilization.

The time-of-flight resonance curve, of both the ion of interest and the reference ion, is measured typically with 21 equidistant frequency steps around the center of the resonance frequency.

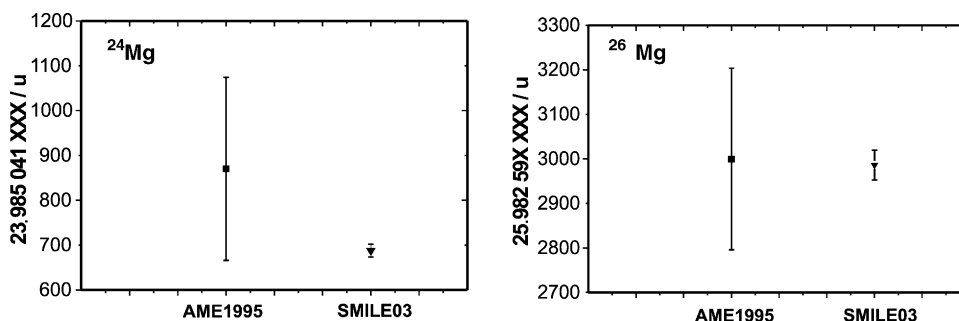


Fig. 2. The mass of the  $^{24}\text{Mg}$  and  $^{26}\text{Mg}$  atoms measured with SMILETRAP Penning trap mass spectrometer compared to the previous best mass values.

One scan, involving 21 frequency steps, takes about 40 s and is repeated twice. After two complete scans the settings are switched between the two ion species; the reference ion  $\text{H}_2^+$  and the ion of interest. To switch between ion species takes only about 1 s, thus the total cycle time is shorter than 3 min. In this way any change in the magnetic field between the measurement of the ion of interest and the reference ion is reduced.

The mass of the ion is obtained from the observed cyclotron frequency ratio of the two ion species:

$$m_1 = \frac{\nu_2 q_1}{\nu_1 q_2} m_2, \quad (1)$$

where the subscript 1 denotes the main ion and subscript 2 the reference ion.

Since the two frequency measurements are performed in similar ways, certain systematic uncertainties in the frequency ratio cancel out to a large extent. This is in particular the case for ions which have the same  $q/A$  value. For a detailed discussion of the systematic errors see Ref. [4].

### 3. Results and discussions

#### 3.1. Mass measurements related to $g$ -factor experiments

The ionic mass is an essential ingredient when evaluating the  $g$ -factor experiments of the bound electron in hydrogen-like and lithium-like ions [14] which aim to make benchmark tests of QED calculations [15]. Investigations of high  $Z$  hydrogen-like systems are strongly restricted by an uncertainty due to nuclear size effects. In the case of the bound electron  $g$ -factor the role of the nuclear effects is not so crucial as in the case of the hyperfine structure splitting. Furthermore, in a certain combination involving differences of the  $g$ -factor of the hydrogen-like and lithium-like ions this can be significantly reduced [16]. The value of  $g$  can be obtained from

$$g = 2 \frac{\omega_L q m_e}{\omega_c e M}, \quad (2)$$

where  $\omega_L$  is the Larmor precession frequency (see, e.g., Ref. [14]),  $m_e$  is the mass of the electron and  $M$  is the mass of the ion under investigation. Both  $\omega_L$  and  $\omega_c$  can be accurately measured in the  $g$ -factor experiment.

So far the hydrogen-like  $^{12}\text{C}^{5+}$  and  $^{16}\text{O}^{7+}$  are the heaviest ions used in the  $g$ -factor experiment. In both cases the ionic mass was accurately known and the dominant part of the uncertainty

in  $g$  was due to the uncertainty in the electron mass. Therefore, from the  $^{12}\text{C}^{5+}$  experiment a new value for the electron mass with four times smaller uncertainty was derived. This could be done since the C atom is the mass standard and the theoretical  $g$ -factor value is trusted with that accuracy. The present relative standard uncertainty in the electron mass is 0.44 ppb [17]. The proposed new  $g$ -factor experiments, involving medium heavy ions like  $^{40}\text{Ca}$  [14], therefore require ion masses with similar uncertainties as in the electron mass.

The masses of  $^{24}\text{Mg}^{11+}$  and  $^{26}\text{Mg}^{11+}$  measured at SMILETRAP for planned  $g$ -factor experiments have been reported in reference [18]. Recently, also the masses of the hydrogen-like and lithium-like  $^{40}\text{Ca}$  ions were measured at SMILETRAP [19]. As a by-product new atomic mass values of  $^{24}\text{Mg}^{11+}$ ,  $^{26}\text{Mg}^{11+}$ , and  $^{40}\text{Ca}$  were obtained as shown in Figs. 2 and 3.

By considering the ratio of  $g$ -factors of hydrogen-like ions of different isotopes of the same element, the dependence on the electron mass can be eliminated. An isotope effect in the  $g$ -factor,  $\Delta g = g_2/g_1 - 1$ , can thus be introduced to characterize this effect. It was shown in Ref. [18] that an isotope effect in the  $g$ -factor would be measurable already between  $^{24}\text{Mg}^{11+}$  and  $^{26}\text{Mg}^{11+}$  thanks to the high precision mass values measured with SMILETRAP for both isotopes. The size of the isotope effect in the  $g$ -factor is more pronounced if the relative difference in the mass is larger, e.g., between  $^{40}\text{Ca}^{19+}$  and  $^{48}\text{Ca}^{19+}$  or between  $^{36}\text{Ar}^{17+}$  and  $^{40}\text{Ar}^{17+}$ . In the theoretical calculation of the  $g$ -factor of the bound electron in hydrogen-like ions the mass has the largest impact on the so-called recoil term  $g_{\text{recoil}}$ . The magnitudes of this term and the isotope effects are calculated to

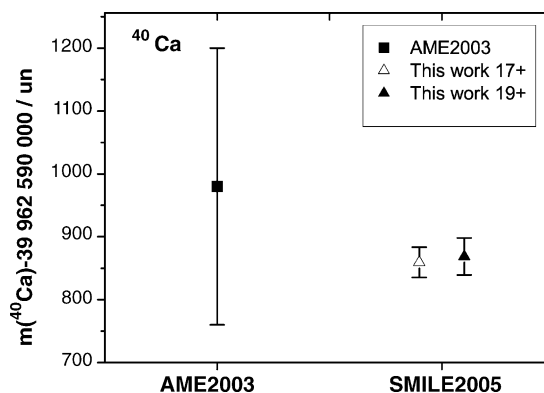


Fig. 3. The mass of  $^{40}\text{Ca}$  derived from measurements of hydrogen-like and lithium-like  $^{40}\text{Ca}$  ions compared to the previous best values.

Table 1

The  $g_{\text{recoil}}$  term calculated to first order and the resulting isotope effect  $\Delta g$  in the  $g$ -factor for two selected isotope pairs (see text)

Isotope	$g_{\text{recoil}}$	$\Delta g$
$^{24}\text{Mg}^{11+}$	$1.75 \times 10^{-7}$	
$^{26}\text{Mg}^{11+}$	$1.62 \times 10^{-7}$	$6.7 \times 10^{-9}$
$^{40}\text{Ca}^{19+}$	$2.92 \times 10^{-7}$	
$^{48}\text{Ca}^{19+}$	$2.43 \times 10^{-7}$	$2.4 \times 10^{-8}$

first order for two hydrogen-like ion pairs using Refs. [18,20,21], and are given in Table 1.

### 3.2. Atomic binding energies from mass measurements

In order to get the atomic mass from the resonance frequency ratio of the probed ion to the reference ion, the mass of the missing electrons have to be added. This is a critical issue, especially when highly charged ions are used and a large number of bound electrons have to be added. The atomic mass  $m_A$  of atom  $A$  is then the ionic mass, corrected for the masses  $qm_e$  of the missing electrons and their total binding energy ( $E_B$ ):

$$m_A = \frac{\nu_2}{\nu_1} \frac{q_1}{q_2} m_2 + qm_e - E_B(A^{q+}), \quad (3)$$

For the binding energies of electrons in highly charged ions, so far, only calculated values exist. In Fig. 4, the binding energies of the last ionized electron for  $\text{Pb}^{q+}$  are plotted. The values were taken from Ref. [22] (open circles), and from Ref. [23] (full circles). It is interesting to notice that the two calculations agree rather well, except in the interval between  $q = 14$  and 36. The discrepancy between the calculations should be far outside their accuracy limits. Accuracy limits for binding energies over such a broad range of charges are difficult to estimate. They should definitely be lower than 100 eV over the whole charge range and for some charge states at shell closure near to 10 eV. To calculate the atomic mass, these binding energies of all individual electrons have to be added up. Systematic uncertainties in the individual binding energies are adding up as well. One gets a rather large difference in the total binding energy between Refs. [22] and [23] for charge states of Pb around 30 (see inset in Fig. 4). It is also evident from Fig. 4 that an ion with an atomic-shell closure has advantages. The contribution from the binding energy makes a large step when opening a new shell, whereas the relative accuracy in the frequency determination changes marginally. The binding-energy calculations also get more accurate (see below) for an ion with a closed shell.

The calculated binding energies are experimentally tested for low degrees of ionization. Otherwise the atomic structure calculations are rather well tested by experimental transition energies over the whole periodic system and charge spectrum. In Ref. [24] calculations for highly charged ions were tested with different methods in their consistency. From there the error limit is derived. These calculations [24] were for closed shell systems on a level of accuracy of 10 eV for medium  $Z$  ions. The uncertainty comes mostly from correlation effects (which are typically around 50–60 eV for Ar-like ions) and from QED effects (in particular the many-body QED contributions). It should

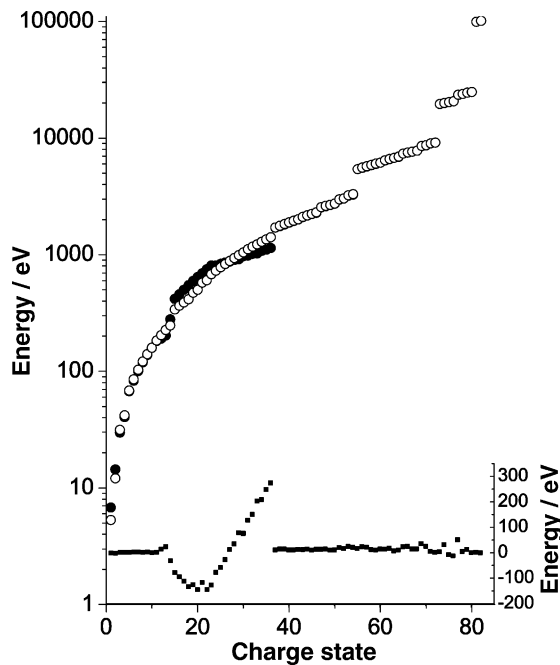


Fig. 4. The binding energies of the last ionized electron for  $\text{Pb}^{q+}$  are plotted. The values were taken from Ref. [22] (open circles), and from Ref. [23] (full circles). The inset, with the scale on the right side, shows the difference between the two calculations over  $q$ .

be noticed that QED contributions get large when coming to alkali-like ions where s-shell electrons are added. In first order, the QED contributions get negligible when one comes to p-shell electrons. The typical contributions to the atomic masses from the total binding energies are (in some examples):  $\text{H}_2^+ E_B = -15.4 \text{ eV} = 8.3 \text{ ppb}$ ,  $^{208}\text{Pb}^{50+} E_B = -50.372 \text{ keV} = 260 \text{ ppb}$ ,  $^{208}\text{Pb}^{72+} E_B = -172.177 \text{ keV} = 889 \text{ ppb}$ .

One can turn this around and by measuring the mass of the same isotope using different ion charges, the binding energy of a number of electrons in the atom can be obtained as a mass difference. This is especially the case when the precision reaches  $\sim 2$ –10 eV or better, so that the influence from correlation, relativistic, Breit, and QED corrections can be directly measured. Some simple Z-scaling rules help to reveal the relative importance of the different contributions over a wide range of  $q$ ,  $Z$ , and  $A$ . Correlation is, for a fixed number of electrons, rather independent of  $Z$  and increases linearly with the electron number by roughly  $2 \text{ eV}/e^-$ . In first order, the binding energy scales with  $Z^2$  and QED with  $Z^4$  and  $n^{-3}$ . The absolute precision decreases linearly with the ion mass. Correlation effects are, relative to QED, most dominant in lighter ions ( $A \sim 50$ ) and medium charges. There a precision of  $10^{-10}$  results in 5 eV which gets sensitive to correlation effects. For measuring QED effects, heavy ions in the highest charge states are required. On top of that a precision of better than  $10^{-10}$  for  $A \sim 200$  is needed. This has not been demonstrated yet but seems achievable in the near future. In particular when measuring charge state sequences such a precision should be achievable in a relative comparison between the ion masses in different charge states.

For the example shown in Fig. 4, one has in the mass difference from Cu-like to Ni-like Pb a QED effect in the order of

Table 2

The mass of a few selected hydrogen-like and lithium-like ions measured with SMILETRAP relevant for the  $g$ -factor experiment

Ion	Mass (u)	Rel. unc. (ppb)
$^{24}\text{Mg}^{11+}$	23.979011054 (17)	0.6
$^{26}\text{Mg}^{11+}$	25.976562347 (32)	1.3
$^{40}\text{Ca}^{19+}$	39.952181819 (29)	0.7
$^{40}\text{Ca}^{17+}$	39.953272223 (24)	0.6

2 eV [25], corresponding to around  $10^{-11}$  of the ion mass difference. For the Li-like to He-like Pb mass difference the QED contribution is around 30 eV [26], and already  $1.5 \times 10^{-10}$ . For H-like Pb one calculates [27] around 245 eV for the QED effect in the 1s state, which makes a mass contribution of 1 ppb. If the  $^{208}\text{Pb}^{81+}$  to  $^{208}\text{Pb}^{82+}$  or  $^{208}\text{Pb}^{80+}$  mass difference could be measured to  $10^{-11}$ , one would have the same accuracy in determining the QED contribution as present day X-ray spectroscopic measurements.

#### 4. Conclusion and outlook

SMILETRAP is in fact so far the only facility where highly charged ions (with  $q > 8+$ ) have been used for mass measurements. It has proven to reach high accuracy in the  $10^{-10}$  range for ions all over the periodic table.

For the  $g$ -factor experiments on hydrogen-like and lithium-like ions, the ionic mass is required (see Eq. (3)) with an uncertainty comparable to the uncertainty in the electron mass (0.44 ppb) or better. Since, in our experiment, the mass of the hydrogen-like or Li-like ion is directly obtained one gets rid of the critical binding energy correction otherwise necessary for mass determinations based on singly charged ions. As seen from Table 2, our best ionic heavy-mass uncertainty (for Ca) is 0.6 ppb. About 0.3 ppb comes from limited statistics. By using Ramsey excitation, carbon ions of suitable charge state as mass reference (to allow for  $q/A$  doublet measurements) and better statistics we hope to get close to 0.1 ppb.

We plan to move SMILETRAP to a new electron beam ion trap (EBIT) located at AlbaNova to have access to higher charge states. At present this source can produce up to neon-like ions of any element. Later an upgrade of the source is planned to a 250 keV electron beam with which fully stripped ions up to  $\text{U}^{92+}$  can be produced. With that configuration we aim at measuring masses for the  $g$ -factor of bound electron in ions such as  $^{238}\text{U}^{91+}$  and weighing directly the QED contribution in the masses of heavy highly charged ions.

#### Acknowledgements

We gratefully acknowledge support from the Knut and Alice Wallenberg Foundation, the European networks EUROTRAP and HITRAP (contract no. HPRI CT 2001 50036), and from the Swedish Research Council VR. We are also indebted to the Manne Siegbahn Laboratory for their support. Last but not least we want to express our most sincere thanks to Juergen Kluge for his support of SMILETRAP from the very beginning.

#### References

- [1] D. Lunney, J.M. Pearson, C. Thibault, *Rev. Mod. Phys.* 75 (2003) 1021.
- [2] G. Bollen, et al., *Nucl. Instrum. Methods A* 368 (1995) 675.
- [3] G. Gräff, H. Kalinowski, J. Traut, *Z. Phys. A* 297 (1980) 35.
- [4] I. Bergström, C. Carlberg, T. Fritioff, G. Douysset, R. Schuch, J. Schönfelder, *Nucl. Instrum. Methods A* 487 (2002) 618.
- [5] G. Douysset, T. Fritioff, C. Carlberg, I. Bergström, M. Björkhage, *Phys. Rev. Lett.* 86 (2001) 4250.
- [6] C. Carlberg, T. Fritioff, I. Bergström, *Phys. Rev. Lett.* 83 (1999) 4506.
- [7] I. Bergström, T. Fritioff, R. Schuch, J. Schönfelder, *Phys. Scr.* 66 (2002) 201.
- [8] T. Fritioff, H. Bluhme, R. Schuch, I. Bergström, M. Björkhage, *Nucl. Phys. A* 723 (2003) 3.
- [9] Sz. Nagy, T. Fritioff, M. Björkhage, I. Bergström, R. Schuch, *Europhys. Lett.*, submitted for publication.
- [10] Sz. Nagy, T. Fritioff, M. Suhonen, R. Schuch, K. Blaum, M. Björkhage, I. Bergström, *Phys. Rev. Lett.*, submitted for publication.
- [11] E. Bebee, et al., *Phys. Scr.* 47 (1993) 470.
- [12] L.S. Brown, G. Gabrielse, *Rev. Mod. Phys.* 58 (1986) 233.
- [13] M. König, et al., *Int. J. Mass Spectrom.* 142 (1995) 95.
- [14] M. Vogel, J. Alonso, S. Djekic, H.-J. Kluge, W. Quint, S. Stahl, J. Verdú, G. Werth, *Nucl. Instrum. Methods B* 235 (2005) 7.
- [15] V.A. Yerokhin, A.N. Artemyev, P. Indelicato, V.M. Shabaev, *Nucl. Instrum. Methods B* 205 (2003) 47.
- [16] V.M. Shabaev, D.A. Glazov, M.B. Shabaeva, V.A. Yerokhin, G. Plunien, G. Soff, *Phys. Rev. A* 65 (2002) 062104.
- [17] P.J. Mohr, B.N. Taylor, *Rev. Mod. Phys.* 77 (2005) 1.
- [18] I. Bergström, M. Björkhage, K. Blaum, H. Bluhme, T. Fritioff, Sz. Nagy, R. Schuch, *Eur. Phys. J. D* 22 (2003) 41.
- [19] Sz. Nagy, T. Fritioff, A. Solders, R. Schuch, M. Björkhage, I. Bergström, *Eur. Phys. J. D*, in press.
- [20] V.M. Shabaev, V.A. Yerokhin, *Phys. Rev. Lett.* 88 (2002) 091801.
- [21] T. Beier, et al., *Phys. Rev. A* 62 (2000) 032510.
- [22] J. Scofield, *Ionisation Energies*, LLNL internal report, Livermore, California 94550, USA (1986).
- [23] G.C. Rodrigues, P. Indelicato, J.P. Santos, P. Patte, F. Parente, *At. Nucl. Data Tables* 86 (2004) 117.
- [24] G.C. Rodrigues, M.A. Ourdane, J. Bieron, P. Indelicato, E. Lindroth, *Phys. Rev. A* 63 (2001) 012510.
- [25] E. Lindroth, M. Tokman, P. Glans, Z. Pesic, G. Viktor, H. Danared, M. Pajek, R. Schuch, *Phys. Rev. Lett.* 86 (2001) 5027.
- [26] S.A. Blundell, *Phys. Rev. A* 47 (1993) 1790.
- [27] W.R. Johnson, G. Soff, *At. Data Nucl. Data Tables* 33 (1985) 405.